Familial Parkinson's point mutation abolishes multiple system atrophy prion replication

Amanda L. Woerman[a,b], Sabeen A. Kazmi[a], Smita Patel[a], Atsushi Aoyagi[a,c], Abby Oehler[a], Kartika Widjaja[a], Daniel A. Mordes[d], Steven H. Olson[a,b], and Stanley B. Prusiner[a,b,e,1]

[a]Institute for Neurodegenerative Diseases, Weill Institute for Neurosciences, University of California, San Francisco, CA 94158; [b]Department of Neurology, University of California, San Francisco, CA 94158; [c]Daiichi Sankyo Co., Ltd., Tokyo 140-8710, Japan; [d]C. S. Kubik Laboratory for Neuropathology, Department of Pathology, Massachusetts General Hospital, Boston, MA 02114; and [e]Department of Biochemistry and Biophysics, University of California, San Francisco, CA 94158

Contributed by Stanley B. Prusiner, November 22, 2017 (sent for review November 7, 2017; reviewed by Jason C. Bartz and Krister Kristensson)

In the neurodegenerative disease multiple system atrophy (MSA), α-synuclein misfolds into a self-templating conformation to become a prion. To compare the biological activity of α-synuclein prions in MSA and Parkinson's disease (PD), we developed nine α-synuclein–YFP cell lines expressing point mutations responsible for inherited PD. MSA prions robustly infected wild-type, A30P, and A53T α-synuclein–YFP cells, but they were unable to replicate in cells expressing the E46K mutation. Coexpression of the A53T and E46K mutations was unable to rescue MSA prion infection in vitro, establishing that MSA α-synuclein prions are conformationally distinct from the misfolded α-synuclein in PD patients. This observation may have profound implications for developing treatments for neurodegenerative diseases.

α-synuclein | neurodegeneration | proteinopathy | strains | synucleinopathies

Multiple system atrophy (MSA) is a rapidly progressing neurodegenerative disease resulting in dysfunction of the autonomic nervous system and disrupted motor function. The pathological hallmark of MSA is the presence of α-synuclein aggregates that coalesce into glial cytoplasmic inclusions (GCIs) in oligodendrocytes (1). MSA is one of four synucleinopathies, the other three being Parkinson's disease (PD), Parkinson's disease with dementia (PDD), and dementia with Lewy bodies (DLB). In PD, PDD, and DLB patients, α-synuclein accumulates in neurons as Lewy bodies and Lewy neurites (2). Recent studies demonstrate that MSA is unequivocally caused by α-synuclein prions, which are misfolded proteins that undergo self-propagation and are capable of transmitting disease to transgenic (Tg) mice (3–6). Using TgM83$^{+/-}$ mice, which express human α-synuclein with the familial A53T mutation, both intracranial (3, 5) and peripheral inoculation (6) of brain homogenate from a total of 17 MSA patients induced neurological disease in the animals. In addition, α-synuclein prions isolated from MSA patients propagated in cultured HEK cells that express mutant human α-synuclein*A53T fused to YFP (α-syn140*A53T–YFP) (4). While PD transmission studies have induced α-synuclein neuropathology (7–9), attempts to transmit disease to TgM83$^{+/-}$ mice or to infect α-syn140*A53T–YFP cells have been unsuccessful (5), suggesting that distinct conformations of misfolded α-synuclein or α-synuclein prion strains may be responsible for these diseases.

To study the strain-specific properties of α-synuclein prions in MSA patients and to reconcile the differences between PD and MSA prions, we conducted a series of studies to investigate the effect of inherited PD point mutations on MSA prion replication. In addition to the original WT (α-syn140–YFP) and α-syn140*A53T–YFP cells first reported in 2015 (4), we generated seven additional HEK cell lines expressing single mutations (A30P and E46K), double mutations (A30P,A53T and E46K,A53T), and truncated α-synuclein*A53T (residues 1–95, 1–97, and 29–97). After measuring MSA prion infection in the WT, A30P, and A53T cell lines, we were surprised to observe that the E46K mutation prevented the replication of MSA prions in vitro. Moreover, coexpressing the E46K and A53T mutations failed to facilitate robust propagation, underscoring the presence of two distinct prion strains in MSA and PD patients. Interestingly, truncation of α-synuclein*A53T at amino acid residue 95, which has been reported to increase the propensity of the protein to aggregate (10), also blocked MSA infection, but the addition of the two lysines at residues 96 and 97 restored MSA prion replication in vitro. The same selective infectivity demonstrated for MSA prions across the α-synuclein–YFP cell lines was observed using both mouse- and cell-passaged MSA samples, arguing that prion replication occurs with high fidelity in the two model systems.

Recombinant or synthetic α-synuclein fibrils are typically used in lieu of patient-derived material in synucleinopathy research. When recombinant α-synuclein fibrils (WT, A30P, E46K, and A53T) were tested on the α-synuclein–YFP cell lines, all four fibrils showed broad, nonselective infection, contending that the conformation(s) present were not representative of MSA prions. Following this observation, we compared the stability of MSA prions with α-synuclein fibrils under two denaturing conditions. We found that while MSA prions were completely degraded by either 5 μg proteinase K (PK) or 3 M guanidine (GnHCl), α-synuclein fibrils were only partially denatured under the same conditions. Together, these results indicate that MSA is caused by a distinct conformation of α-synuclein prions compared with PD and that neither of these conformations is well represented by α-synuclein fibrils.

Significance

In Parkinson's disease (PD) and multiple system atrophy (MSA), the accumulation and spread of α-synuclein prions leads to the progressive degeneration seen in patients. These diseases are thought to arise from unique conformations of α-synuclein prions—or strains. To investigate this hypothesis, we infected cell lines expressing PD-causing point mutations in α-synuclein with MSA patient samples. Unexpectedly, the E46K mutation inhibited MSA prion replication. This observation indicates that the α-synuclein prion conformation found in PD is different from the strain found in MSA, providing biological evidence that these diseases arise from distinct prion strains. The ability of α-synuclein recombinant fibrils to infect all cell lines tested argues that synthetic α-synuclein prions are not predictive of the disease-causing strains in human patients.

Author contributions: A.L.W., S.H.O., and S.B.P. designed research; A.L.W., S.A.K., S.P., A.O., and D.A.M. performed research; A.A. and K.W. contributed new reagents/analytic tools; A.L.W., S.A.K., S.P., S.H.O., and S.B.P. analyzed data; and A.L.W., S.H.O., and S.B.P. wrote the paper.

Reviewers: J.C.B., Creighton University; and K.K., Karolinska Institutet.

Conflict of interest statement: The Institute for Neurodegenerative Diseases has a research collaboration with Daiichi Sankyo (Tokyo, Japan). S.B.P. is the chair of the Scientific Advisory Board of Alzheon, Inc., which has not contributed financial or any other support to these studies.

[1]To whom correspondence should be addressed. Email: stanley.prusiner@ucsf.edu.

This article contains supporting information online at www.pnas.org/lookup/suppl/doi:10.1073/pnas.1719369115/-/DCSupplemental.

Results

Cell-Passaged MSA Prions Transmit Disease to TgM83$^{+/-}$ Mice. Following our initial observation that α-synuclein prions isolated from MSA patients infect HEK cells expressing the α-syn140*A53T–YFP fusion protein, we developed additional HEK cell lines expressing WT (α-syn140–YFP) and A30P-mutated α-synuclein (α-syn140*A30P–YFP) to compare the effect of disease-causing mutations on α-synuclein prion replication (Fig. S1 and Table S1). α-Synuclein prions were isolated from brain homogenate prepared from one control (C2) and three MSA patients (MSA12, MSA13, and MSA14) by precipitation with phosphotungstic acid (PTA) (4) and were incubated with α-syn140–YFP, α-syn140*A30P–YFP, and α-syn140*A53T–YFP cells in a 384-well plate for 4 d. Live cells were imaged using the IN Cell Analyzer 6000 cell-imaging system (GE Healthcare), and the images were analyzed to determine the total fluorescence in the aggregates divided by the cell count (fluorescence/cell × 10^3 a.u.). For each sample, five images were collected from six wells. A single value was determined for each well, and the six technical replicates were averaged for each sample. While C2 had no effect on the three lines (Fig. 1*A* and Table S2), MSA prions significantly infected α-syn140–YFP ($P = 0.0001$), α-syn140*A30P–YFP (MSA12, $P = 0.0009$; MSA13, $P = 0.0001$; MSA14, $P = 0.0003$), and α-syn140*A53T–YFP cells ($P = 0.0001$), inducing the formation of YFP$^+$ aggregates in the cells. Notably, infection in the α-syn140*A53T–YFP cells was more robust than in the cells expressing WT or A30P-mutated α-synuclein, which were similarly infected by the three samples.

Recognizing that MSA prions can be serially propagated in the α-syn140*A53T–YFP cells (4), we tested the ability of the infected cells to transmit disease to mice. After infecting α-syn140*A53T–YFP cells with MSA prions isolated from patient MSA14, we isolated two stable clones containing α-synuclein–YFP aggregates (MSA14-11 and MSA14-12). A third clone was produced by infecting cells expressing truncated mutant human α-synuclein (α-syn95*A53T–YFP) (Table S1) with lysate collected from the MSA-infected α-syn140*A53T–YFP cells (MSA14-M1). Lysates collected from all three clones, as well as three separate preparations of uninfected α-syn140*A53T–YFP cells, were inoculated intracerebrally into TgM83$^{+/-}$ mice (Fig. 1 *B* and *C*). Lysates from MSA14-12 and MSA14-M1 transmitted neurological disease to all the inoculated animals (173 ± 70 d, $n = 7$ and 177 ± 50 d, $n = 8$, respectively), and MSA14-11 transmitted disease to five of seven mice within 400 d (incubation time for symptomatic animals, 227 ± 95 d) (Fig. 1*B*). None of the 19 total mice inoculated with uninfected lysate developed disease within 400 d, indicating that uninfected α-syn140*A53T–YFP cells do not develop spontaneous α-synuclein prions ($P < 0.0001$). Moreover, we found that frozen half-brains from symptomatic mice contained α-synuclein prions, as measured in the α-syn140*A53T–YFP cell assay (MSA12, 65 ± 27 × 10^3 a.u.; MSA13, 76 ± 20 × 10^3 a.u.; 98 ± 20 × 10^3 a.u.; $P = 0.0001$), but prions were not detected in the control mice (2.7 ± 0.7 × 10^3 a.u.) (Fig. 1*C*). Symptomatic animals inoculated with the MSA lysates developed phosphorylated α-synuclein neuropathology (antibody for pS129) and astrogliosis in the diencephalon and brainstem (Fig. S2). Analogous to α-synuclein aggregates in MSA patients, pS129 immunostaining colocalized with both p62 (Fig. S2*B*) and ubiquitin (Fig. S2*C*). These findings indicate that the YFP$^+$ aggregates induced by MSA prions in the α-synuclein–YFP cells are neuropathogenic.

MSA Prion Replication Is Blocked by the PD E46K Mutation. After observing MSA prion replication in α-synuclein–YFP cells expressing WT, A30P, and A53T α-synuclein, we tested infection in cells expressing the E46K mutation (α-syn140*E46K–YFP). Unexpectedly, we found that MSA prions were unable to infect the E46K-expressing cells ($P = 0.25$) (Fig. 2*A* and Table S2) despite evidence that the mutation gives rise to familial PD and DLB (11). When we coexpressed both the E46K and A53T mutations in the same cell line (α-syn140*E46K,A53T–YFP), the MSA prions showed a significant infection in the cells compared with the control sample (MSA12 and MSA13, $P = 0.0001$; MSA14, $P = 0.01$). The magnitude of infection, however, was substantially reduced compared with the α-syn140*A53T–YFP cells. Notably, when we coexpressed the A30P and A53T mutations (α-syn140*A30P,A53T–YFP), we observed robust infection with MSA prions ($P = 0.0001$), indicating that the stunted replication in the α-syn140*E46K,A53T–YFP cells is a result of the observed dominant inhibition of the E46K mutation.

The 3D structure of α-synuclein prions isolated from an MSA patient has not been determined. Crystal structures of misfolded proteins from neurodegenerative disease patient samples are

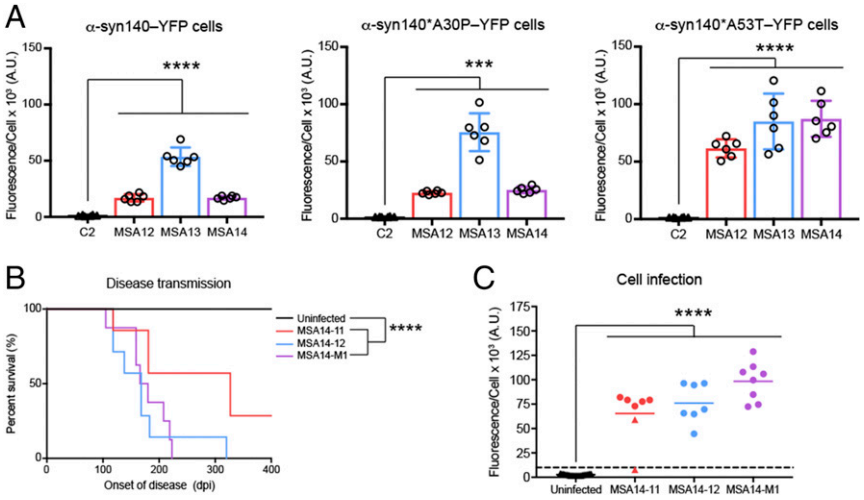

Fig. 1. Cell-passaged MSA prions transmit disease. (*A*) α-Synuclein prions were isolated from three MSA patient samples and one control sample by phosphotungstic acid precipitation. The MSA prions were able to significantly infect HEK cells expressing WT and mutated (A30P and A53T) α-synuclein–YFP fusion proteins. Data are shown as mean ± SD. (*B* and *C*) Patient sample MSA14 was used to generate stable clones infected with MSA prions (MSA14-11, MSA14-12, and MSA14-M1). Lysates from infected and uninfected cells were inoculated into TgM83$^{+/-}$ mice (30 μg protein). (*B*) The Kaplan–Meier plot shows the onset of neurological signs. Dpi, days post inoculation. (*C*) α-Synuclein prions were measured from frozen half-brains in the α-syn140*A53T–YFP cell assay (× 10^3 a.u.). Circles indicate infected mice that died from disease (above dotted line); triangles indicate asymptomatic animals terminated 400 d post inoculation. Mice inoculated with cell-passaged MSA contained significantly more α-synuclein prions than controls. ***$P < 0.001$, ****$P < 0.0001$.

not feasible to generate, and only recently has cryo-electron microscopy (cryo-EM) enabled structural biologists to ascertain the structure of tau prions from an Alzheimer's disease patient (12). A handful of α-synuclein structures have been reported using synthetic fibrils, although many are based on highly ordered protein fragments (13–16). Comparing our finding that the E46K mutation blocks MSA prion replication with the published α-synuclein structures, we noted that the Greek key motif proposed by Tuttle et al. (13), which is based on a solid-state NMR structure of full-length fibrils, suggests that residue E46 forms an important salt bridge with K80 to stabilize the conformation. In this structure, the mutation at residue 46 to a lysine would result in a repulsive interaction with the lysine at residue 80, disfavoring the conformation. This alteration is consistent with the inability of the A53T mutation to rescue the effects of the E46K mutation in vitro.

Inclusion of lysines 96 and 97 in the highly ordered region of the α-synuclein model proposed by Tuttle et al. (13) is in contrast with the systemic mutagenesis studies that showed truncating α-synuclein at residue 95 increases the propensity of the protein to aggregate in vitro (10). Testing the effect of both of these truncations on MSA prion replication, we created HEK cells expressing A53T-mutated human α-synuclein shortened to either 95 residues (α-syn95*A53T–YFP) or 97 residues (α-syn97*A53T–YFP) (Fig. 2*B*). After incubating both cell lines with MSA prions, we measured a minute increase in aggregate formation in the α-syn95*A53T–YFP cells (MSA12 and MSA13, $P = 0.0001$; MSA14, $P = 0.02$) but a robust infection in the α-syn97*A53T–YFP cells (MSA12 and MSA13, $P = 0.0001$; MSA14, $P = 0.001$), suggesting that the MSA prion conformation also requires the two additional lysines for stability. The proposed templating region of α-synuclein in the Greek key structure spans amino acid residues 29–97 (13). In a third cell line expressing this fragment of the protein (α-syn29-97*A53T–YFP), MSA12 and MSA13 induced significant aggregate formation ($P = 0.0001$), but MSA14 did not ($P = 1.0$).

MSA Prions Retain Exquisite Selectivity in α-Synuclein–YFP Cells After Passaging. Comparing the cell-infection data measured from the α-synuclein–YFP cell lines (Figs. 1*A* and 2), we created an infection profile to represent the selective infection of MSA prions across the nine cell lines (Fig. 3*A*). Using brain homogenate from the same MSA patient samples, TgM83$^{+/-}$ mice inoculated with 1% homogenate developed neurological signs (MSA12, 117 ± 27 d, $n = 8$; MSA13, 113 ± 26 d, $n = 8$; MSA14, 130 ± 30 d, $n = 6$; $P < 0.0001$) accompanied by α-synuclein prion formation (MSA12, 52 ± 24 × 10^3 a.u., $n = 5$; MSA13, 52 ± 22 × 10^3 a.u., $n = 5$; MSA14, 68 ± 22 × 10^3 a.u., $n = 4$; $P < 0.0001$) and neuropathology. None of these measures of disease were observed in C2-inoculated animals (terminated 365 d post inoculation, $n = 10$; C2 cell infectivity, 1.8 ± 0.5 × 10^3 a.u., $n = 10$) (Fig. S3). α-Synuclein prions isolated from the brains of two mice inoculated with one of the four patient samples were incubated with the nine α-synuclein–YFP cell lines (Fig. 3*B* and Table S2). The infection profile of the mouse-passaged MSA samples exhibited the same infection bias as the MSA samples across the cell lines, with the E46K mutation and truncation at residue 95 blocking prion replication in vitro. Additionally, the lysates developed from patient sample MSA14 were similarly selective, with minor differences in the WT and A30P cell lines (Fig. 3*C*). However, those differences disappeared when we infected the cells with α-synuclein prions isolated from the brains of four mice inoculated with each lysate (Fig. 3*D*). Importantly, these observations are not due to differences in protein expression across the nine cell lines, given that the cell infectivity pattern is distinct from the measured protein expression in each cell line (Fig. S1). These findings suggest that MSA α-synuclein prions template with high fidelity in TgM83$^{+/-}$ mice and α-synuclein–YFP cells and provide key data about the structure of MSA prions.

α-Synuclein Fibrils Universally Infect α-Synuclein–YFP Cells. The majority of research focusing on α-synuclein misfolding in animal and cellular models of synucleinopathy has relied on recombinant or synthetic α-synuclein that is fibrillized in the laboratory (reviewed in refs. 17–19). To profile the infectivity of synthetic fibrils, we aggregated recombinant WT, A30P, E46K, and A53T α-synuclein and tested serial dilutions of these fibrils for their ability to infect the nine α-synuclein–YFP cell lines (Fig. 4 and Table S2). In seven of the nine cell lines, WT fibril infection was the most robust, with the mutant proteins inducing less aggregate formation. However, in the α-syn140*E46K–YFP and α-syn140*E46K,A53T–YFP cells, the E46K fibrils were the most infectious. Remarkably, all four fibril types infected the α-synuclein–YFP cell lines. In contrast with MSA or passaged MSA prions, synthetic α-synuclein prions showed no discernable infection selectivity in the cell assay (Table 1).

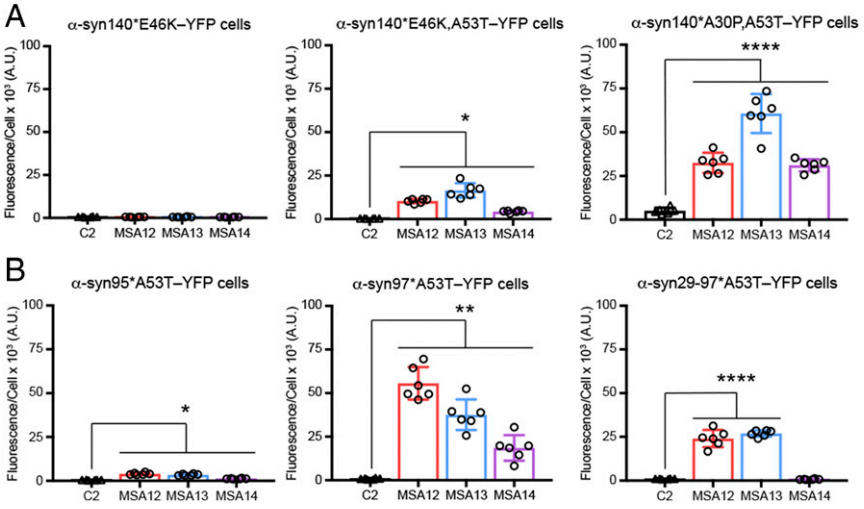

Fig. 2. The E46K mutation in α-synuclein ablates replication of MSA prions. α-Synuclein prions were isolated from three MSA patient samples and one control sample by phosphotungstic acid precipitation and were incubated with HEK cells expressing mutated and truncated α-synuclein–YFP fusion proteins. (*A*) MSA prions were unable to replicate in cells expressing the E46K mutation. Coexpression with the A53T mutation marginally improved infection. However, coexpression of the A30P and A53T mutations resulted in robust replication of MSA prions. (*B*) Truncation of α-syn*A53T at residue 95, but not at residue 97, hindered MSA prion infection in the HEK cells. Data are shown as mean ± SD. *$P < 0.05$, **$P < 0.01$, ****$P < 0.0001$.

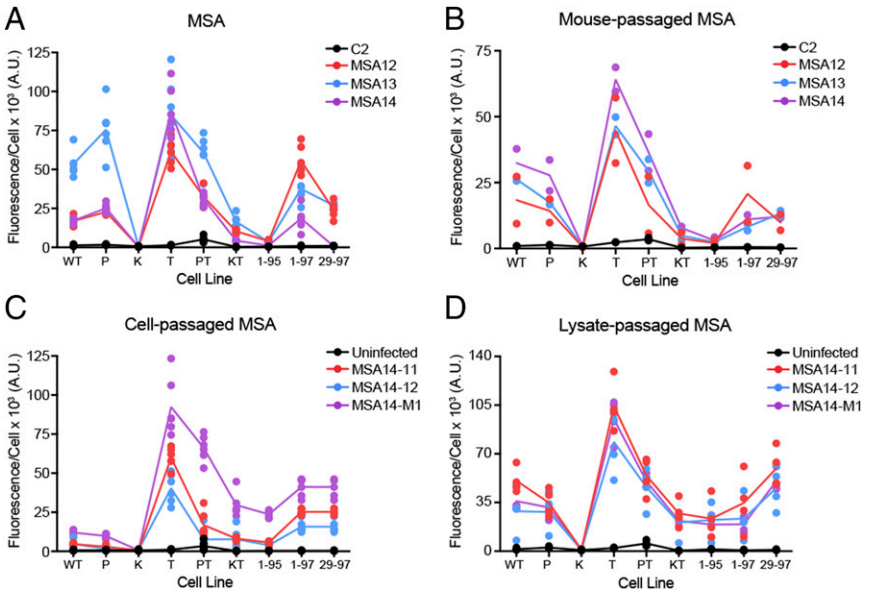

Fig. 3. MSA prions replicate with high fidelity in mice and cells. The nine α-synuclein–YFP cell lines were tested for infection with MSA and passaged MSA homogenates. Cell line abbreviations are given in Table S1. (*A*) MSA prions from patients MSA12, MSA13, and MSA14 were unable to infect cells containing the E46K mutation alone (K) or in combination with the A53T mutation (KT), nor could they infect cells expressing α-synuclein*A53T truncated at residue 95 (1-95). (*B*) MSA prions passaged through TgM83$^{+/-}$ mice showed similar selectivity in the α-synuclein–YFP cell assays. (*C* and *D*) Patient sample MSA14 was used to generate stable clones infected with MSA prions (MSA14-11, MSA14-12, and MSA14-M1). Lysates from these cells showed a similar infectivity profile in the α-synuclein cell lines (*C*), as did TgM83$^{+/-}$ mice inoculated with the lysates (*D*). Control samples did not infect the cells. Data are shown as the mean.

Biochemical Stability of α-Synuclein Prions Is Strain-Dependent. Observing the stark contrast between the infection profile of MSA prions and α-synuclein fibrils, we compared α-synuclein prion stability under denaturing conditions (Figs. S4–S7). To confirm that the α-synuclein prions detected in MSA-inoculated mice templated the misfolded conformation in human patient samples with high fidelity, we first determined the stability of MSA α-synuclein prions using both PK digestion and GnHCl denaturation. While no phosphorylated α-synuclein was detected in C2 brain homogenate, α-synuclein prions in MSA patient samples were resistant to 1 μg PK and were partially resistant to 2.5 μg PK but were fully digested with 5 μg PK at 37 °C for 30 min (Fig. S4). The same resistance to PK digestion was observed in TgM83$^{+/-}$ mice inoculated with MSA homogenates, but no resistance was seen in C2-inoculated animals. However, while 5 μg PK completely digested α-synuclein in MSA patient samples, the same concentration only partially digested all four α-synuclein fibrils (Fig. S5).

Using increasing concentrations of GnHCl to denature the MSA prions, we found no GnHCl-resistant α-synuclein in the C2 homogenate or in TgM83$^{+/-}$ mice inoculated with C2 homogenate (Fig. S6). However, α-synuclein in the MSA patient samples was resistant to 1 M GnHCl but was almost completely denatured by 3 M GnHCl. A similar resistance to GnHCl denaturation was observed in two TgM83$^{+/-}$ mice inoculated with MSA, with resistance to 1 M GnHCl (MSA12, 100 ± 5.4% of control; MSA13, 94 ± 13% of control; MSA14, 100 ± 20% of control) and almost complete degradation by 3 M GnHCl (MSA12, 9.3 ± 4.1% of control; MSA13, 5.9 ± 5.8% of control; MSA14, 7.7 ± 1.3% of control) (dotted lines in Fig. S6*A*). In contrast, 3 M GnHCl denatured only ∼50% of the α-synuclein fibrils [WT, 62% of control; A30P, 49% of control; E46K, 52% of control; A53T, 46% of control (Fig. S7)]. Combined with the cell assay data, these denaturation results establish that α-synuclein fibrils are not entirely representative of the α-synuclein prions in MSA patients. While the fibrils may be composed of one conformation that is distinct from the MSA prion conformation, we cannot rule out the possibility that multiple conformations may be present in each fibril preparation.

Discussion

In the studies reported here, we demonstrate that the misfolded α-synuclein conformation in MSA patients is propagated with high fidelity in cultured cells and TgM83$^{+/-}$ mice. Moreover, the inability of the MSA samples to infect the α-syn140*E46K–YFP cells provides additional evidence that the α-synuclein prion strain that gives rise to MSA is distinct from at least one strain responsible for PD and DLB. Critically, the exquisite selectivity of MSA prions to infect α-synuclein–YFP cells and the lack of PD and DLB sample infection in α-syn140*A53T–YFP cells (4) emphasize that recombinant α-synuclein fibrils are insufficient to serve as a proxy for natural, disease-causing α-synuclein prion strains in research models.

The importance of using strain-specific models of neurodegenerative disease is underscored by a decade of research focused on drug discovery for Creutzfeldt–Jakob disease (CJD). The continued inability to propagate prions from CJD patients in cultured cells currently renders high-throughput screening (HTS) against CJD prions impossible. Instead, HTS campaigns have relied on mouse-adapted scrapie strains, most notably the RML isolate (reviewed in ref. 20). Screening against RML in cultured cells has identified several compounds that significantly extend the life spans of RML-inoculated mice. However, the same compounds were ineffective in mice inoculated with CJD prions (21). This crucial observation highlights the challenges that strain specificity contributes to developing successful therapeutics for all prion diseases.

To overcome this hurdle, the ongoing efforts to bring treatments for synucleinopathy patients to the clinic must rely on model systems that are predictive of the target patient population. One of the more commonly used animal models, the homozygous TgM83 mouse line, develops spontaneous disease around 1 y of age (22). Intracerebral inoculation of brain homogenate from aged, symptomatic animals into 2-mo-old TgM83$^{+/+}$ mice reduced the onset of disease to ∼130 d post inoculation (23, 24), demonstrating the formation of transmissible α-synuclein prions in the animal model. Notably, when the hemizygous TgM83$^{+/-}$ mice were inoculated with homogenate from symptomatic TgM83$^{+/+}$ animals, the incubation period was greatly extended relative to inoculation of brain homogenate from MSA patients (3, 5).

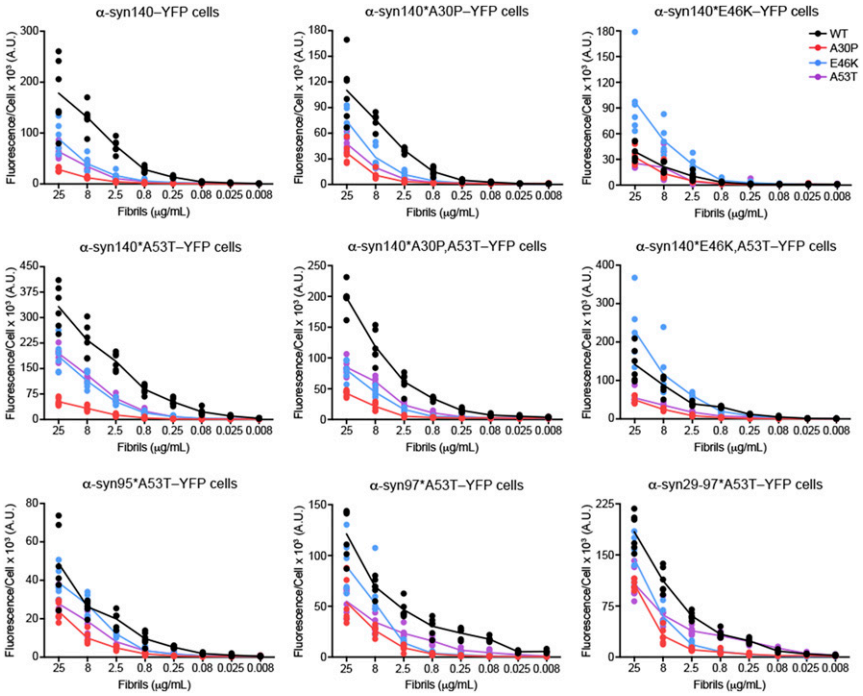

Fig. 4. α-Synuclein fibrils universally infect α-synuclein–YFP cells. WT and mutated (A30P, E46K, and A53T) α-synuclein was fibrillized in 1× DPBS. Serial dilutions of the fibrils, starting with 25 μg/mL protein, were incubated with the nine α-synuclein–YFP cell lines for 4 d. While WT fibrils were the most infectious across seven of the cell lines, the E46K fibrils were the most infectious in the α-syn140*E46K–YFP and α-syn140*E46K,A53T–YFP cell lines. Data are shown as mean.

Distinct prion strains are known to induce differences in incubation period following inoculation, supporting the notion that TgM83$^{+/+}$ mice and MSA patients develop two separate strains of α-synuclein prions. Moreover, inoculation studies testing transmission of disease from PD patients to TgM83$^{+/-}$ mice have failed to induce neurological disease (5), suggesting that PD patients develop a third α-synuclein prion strain.

Providing additional support for this hypothesis, the identification of distinct pathognomonic α-synuclein pathology along with unique symptoms in PD and MSA patients has contributed to the understanding that different conformations of misfolded α-synuclein are responsible for these diseases (5, 25–28). The finding reported here that the E46K mutation, which gives rise to familial PD and DLB (11), obstructs the propagation of MSA prions in cultured cells provides remarkable evidence that MSA is caused by a unique α-synuclein prion strain. Furthermore, mouse- and cell-passaged MSA prions retained the biological properties of human MSA prions, indicating that replication of the strain in both model systems occurs with high fidelity. Recombinant α-synuclein fibrils, however, were found to behave differently from MSA prions. Regardless of whether the fibrils were WT or mutated, they infected all nine α-synuclein–YFP cell lines and exhibited an altered stability to PK digestion and GnHCl denaturation. While it has not been feasible to obtain structural data from patient-derived tissue, it is hoped that recent advances with cryo-EM will provide an opportunity to further investigate strain differences in synucleinopathy patients.

Ongoing efforts to develop effective therapeutics and successful diagnostic tools for PD and MSA patients have largely relied on the use of synthetic or recombinant fibrils. This approach, however, ignores the important discrepancies between the α-synuclein prion strains that give rise to the two diseases. Strain differences likely contribute to a number of central distinctions between PD and MSA, including the cell types affected and the cellular pathways involved. The lessons learned from CJD drug-discovery efforts highlight the importance of strain specificity in therapeutic development. Because α-synuclein fibrils do not fully represent human conformations of α-synuclein prions or differentiate between strains, current efforts focused on developing therapeutics and diagnostics may not translate into useful clinical tools. Instead, replication of MSA prions with high fidelity following inoculation in TgM83$^{+/-}$ mice provides a unique opportunity to evaluate the effect of a compound on human α-synuclein prion propagation in vivo. The ability to propagate a disease-relevant prion strain in cultured cells and Tg mice offers a significant approach to synucleinopathy drug discovery.

Materials and Methods

Human Tissue Samples and Neuropathology. MSA patient samples were obtained from the Massachusetts Alzheimer's Disease Research Center Brain Bank and were assessed to confirm the diagnosis of MSA. Fresh brains were

Table 1. The E46K mutation in α-synuclein prevents propagation of MSA prions, but lysines 96 and 97 are required to stabilize the MSA conformation

Sample	WT	A30P	E46K	A53T	A30P,A53T	E46K,A53T	1-95*A53T	1-97*A53T	29-97*A53T
Control samples	–	–	–	–	–	–	–	–	–
MSA prions	+	+	–	+	+	–	–	+	+
MSA prions → M83$^{+/-}$ mice	+	+	–	+	+	–	–	+	+
MSA prions → α-syn–YFP cells	+	+	–	+	+	–	–	+	+
MSA prions → α-syn–YFP cells → M83$^{+/-}$ mice	+	+	–	+	+	–	–	+	+
WT fibrils	+	+	+	+	+	+	+	+	+
A30P fibrils	+	+	+	+	+	+	+	+	+
E46K fibrils	+	+	+	+	+	+	+	+	+
A53T fibrils	+	+	+	+	+	+	+	+	+

dissected down the midline. One half was fixed in 10% (vol/vol) neutral buffered formalin and coronally sectioned, and the other half was coronally sectioned before rapid freezing. The fixed tissue was evaluated histologically using a set of blocked regions representative of a variety of neurodegenerative diseases. All blocks were stained with Luxol fast blue and H&E. Selected blocks were immunostained for α-synuclein, β-amyloid, and phosphorylated tau. A confirmed MSA diagnosis required the presence of GCIs (29). Control tissue was provided by Martin Ingelsson, Uppsala University, Uppsala, Sweden.

Mice. Animals were maintained in an Association for Assessment and Accreditation of Laboratory Animal Care International-accredited facility in accordance with the *Guide for the Care and Use of Laboratory Animals* (30). All procedures for animal use were approved by the University of California, San Francisco's Institutional Animal Care and Use Committee. All animals were maintained under standard environmental conditions with a 12:12-h light: dark cycle and free access to food and water. To generate the hemizygous TgM83$^{+/-}$ mice, homozygous TgM83$^{+/+}$ mice (22), which express mutated human α-synuclein (A53T) on a B6;C3 background, were purchased from the Jackson Laboratory and were bred with B6C3F1 mice.

Cell Line Development and Lysate Production. Generation of α-syn140−YFP and α-syn140*A53T−YFP cells was previously reported (4). Identical methods were used to develop the additional α-synuclein−YFP cell lines described here.

Monoclonal subclones stably propagating α-synuclein prions following infection with the MSA14 patient sample were generated by isolating α-syn140*A53T−YFP cells by limiting dilution of a polyclonal cell population in 384-well plates. This resulted in the production of clones MSA14-11 and MSA14-12. However, cells expressing full-length synuclein poorly maintained infection. To produce a monoclonal cell line with improved stability, lysate from the previously reported clone MSA14-5 (4) was used to infect α-syn95*A53T−YFP cells, which had poor infection efficiency but produced enough infected cells to develop clone MSA14-M1 via limiting dilution in 384-well plates.

Cell lysates were prepared by harvesting the cells in 1× protease inhibitor (Sigma) diluted in calcium- and magnesium-free 1× Dulbecco's PBS (DPBS). Cell scrapers were used to detach cells from the flask. The resulting cell suspension was placed in sterile conical tubes and frozen at −80 °C overnight. Lysates were thawed quickly at 37 °C and were centrifuged at 500 × *g* for 5 min, and the supernatant was collected. The samples were then centrifuged at 1,000 × *g* for 5 min, and the protein concentration of the supernatant was determined using the bicinchoninic acid (BCA) assay (Pierce).

Fibril Formation. Recombinant α-synuclein monomers (WT, A30P, E46K, and A53T; Sigma) were prepared as previously reported (4). Briefly, protein was suspended in 1× DPBS (concentration of 5 mg/mL) and incubated at 37 °C with constant agitation (1,200 rpm) in an orbital shaker for 7 d. Fibrils were diluted with 1× DPBS to 0.5 mg/mL and stored at 4 °C.

Cell Aggregation Assay. HEK293T cells expressing α-syn140*A53T–YFP were previously reported, and culture and assay conditions were used as described (4). Briefly, α-syn140*A53T–YFP cells were cultured and plated in 1× DMEM supplemented with 10% (vol/vol) FBS, 50 units/mL penicillin, and 50 μg/mL streptomycin (Thermo Fisher). Cells were maintained in a humidified atmosphere of 5% CO_2 at 37 °C. To determine transmission of α-synuclein prions to TgM83$^{+/-}$ mice, α-syn140*A53T–YFP cells were plated at a density of 2,500 cells per well in a 384-well plate with black polystyrene walls (Greiner) with 0.012 μg per well of Hoechst 33342. Plates were returned to the incubator for 2–4 h. Lipofectamine 2000 (1.5% final volume; Thermo Fisher) was incubated with each sample for 1.5 h at room temperature before adding OptiMEM (78.5% final volume; Thermo Fisher). Samples were then added to the α-syn140*A53T–YFP cells in six replicate wells. After the plates were incubated for 4 d at 37 °C in a humidified atmosphere with 5% CO_2, individual plates were imaged using the IN Cell Analyzer 6000 cell-imaging system (GE Healthcare). DAPI and FITC channels were used to collect two images from five different regions in each well. Raw images were analyzed with the IN Cell Developer software (GE Healthcare) using an algorithm designed to detect intracellular aggregates using pixel intensity and size thresholds in living cells, quantified as total fluorescence per cell $\times 10^3$ a.u.

Similar plating conditions were used to compare cell infection using human, mouse-passaged, cell-passaged, and lysate-passaged samples with α-synuclein fibrils. Cells were plated at a cell density of 3,000 cells per well (α-syn140*A53T−YFP), 3,500 cells per well (α-syn140−YFP, α-syn140*E46K−YFP, α-syn140*KT−YFP, and α-syn95*A53T−YFP), or 4,000 cells per well (α-syn140*A30P−YFP, α-syn140*PT−YFP, α-syn97*A53T−YFP, and α-syn29-97*A53T−YFP). Human and mouse samples were diluted 1:10 in 1× DPBS. Lysate samples were plated at a final concentration of 0.1 μg protein per well. Fibrils were first diluted to a final concentration of 25 μg/mL, and seven additional half-log dilutions were also prepared in 1× DPBS.

ACKNOWLEDGMENTS. We thank the Hunters Point animal facility staff for breeding and caring for the mice used in this study and Martin Ingelsson (Uppsala University) for providing control tissue. This work was supported by NIH Grants AG002132 and AG031220, as well as by the Dana Foundation, the Glenn Foundation, the Sherman Fairchild Foundation, the Henry M. Jackson Foundation, Daiichi Sankyo, and the Mary Jane Brinton Fund. The Massachusetts Alzheimer's Disease Research Center is supported by NIH Grant AG005134.

1. Spillantini MG, et al. (1998) Filamentous α-synuclein inclusions link multiple system atrophy with Parkinson's disease and dementia with Lewy bodies. *Neurosci Lett* 251: 205–208.
2. Spillantini MG, et al. (1997) Alpha-synuclein in Lewy bodies. *Nature* 388:839–840.
3. Watts JC, et al. (2013) Transmission of multiple system atrophy prions to transgenic mice. *Proc Natl Acad Sci USA* 110:19555–19560.
4. Woerman AL, et al. (2015) Propagation of prions causing synucleinopathies in cultured cells. *Proc Natl Acad Sci USA* 112:E4949–E4958.
5. Prusiner SB, et al. (2015) Evidence for α-synuclein prions causing multiple system atrophy in humans with parkinsonism. *Proc Natl Acad Sci USA* 112:E5308–E5317.
6. Woerman AL, et al. (2017) MSA prions exhibit remarkable stability and resistance to inactivation. *Acta Neuropathol*, 10.1007/s00401-017-1762-2.
7. Recasens A, et al. (2014) Lewy body extracts from Parkinson disease brains trigger α-synuclein pathology and neurodegeneration in mice and monkeys. *Ann Neurol* 75: 351–362.
8. Masuda-Suzukake M, et al. (2013) Prion-like spreading of pathological α-synuclein in brain. *Brain* 136:1128–1138.
9. Shimozawa A, et al. (2017) Propagation of pathological α-synuclein in marmoset brain. *Acta Neuropathol Commun* 5:12.
10. Burré J, Sharma M, Südhof TC (2012) Systematic mutagenesis of α-synuclein reveals distinct sequence requirements for physiological and pathological activities. *J Neurosci* 32:15227–15242.
11. Zarranz JJ, et al. (2004) The new mutation, E46K, of α-synuclein causes Parkinson and Lewy body dementia. *Ann Neurol* 55:164–173.
12. Fitzpatrick AWP, et al. (2017) Cryo-EM structures of tau filaments from Alzheimer's disease. *Nature* 547:185–190.
13. Tuttle MD, et al. (2016) Solid-state NMR structure of a pathogenic fibril of full-length human α-synuclein. *Nat Struct Mol Biol* 23:409–415.
14. Vilar M, et al. (2008) The fold of α-synuclein fibrils. *Proc Natl Acad Sci USA* 105: 8637–8642.
15. Atsmon-Raz Y, Miller Y (2015) A proposed atomic structure of the self-assembly of the non-amyloid-β component of human α-synuclein as derived by computational tools. *J Phys Chem B* 119:10005–10015.
16. Rodriguez JA, et al. (2015) Structure of the toxic core of α-synuclein from invisible crystals. *Nature* 525:486–490.
17. Hasegawa M, Nonaka T, Masuda-Suzukake M (2016) α-Synuclein: Experimental pathology. *Cold Spring Harb Perspect Med* 6:a024273.
18. Tofaris GK, Goedert M, Spillantini MG (2017) The transcellular propagation and intracellular trafficking of α-synuclein. *Cold Spring Harb Perspect Med* 7:a024380.
19. Burré J, Sharma M, Südhof TC (2017) Cell biology and pathophysiology of α-synuclein. *Cold Spring Harb Perspect Med* 7:a024091.
20. Giles K, Olson SH, Prusiner SB (2017) Developing therapeutics for PrP prion diseases. *Cold Spring Harb Perspect Med* 7:a023747.
21. Giles K, et al. (2010) Human prion strain selection in transgenic mice. *Ann Neurol* 68: 151–161.
22. Giasson BI, et al. (2002) Neuronal α-synucleinopathy with severe movement disorder in mice expressing A53T human α-synuclein. *Neuron* 34:521–533.
23. Mougenot A-L, et al. (2012) Prion-like acceleration of a synucleinopathy in a transgenic mouse model. *Neurobiol Aging* 33:2225–2228.
24. Luk KC, et al. (2012) Intracerebral inoculation of pathological α-synuclein initiates a rapidly progressive neurodegenerative α-synucleinopathy in mice. *J Exp Med* 209: 975–986.
25. Goedert M (2015) Neurodegeneration. Alzheimer's and Parkinson's diseases: The prion concept in relation to assembled Aβ, tau, and α-synuclein. *Science* 349:1255555.
26. Prusiner SB (2012) Cell biology. A unifying role for prions in neurodegenerative diseases. *Science* 336:1511–1513.
27. Peelaerts W, et al. (2015) α-Synuclein strains cause distinct synucleinopathies after local and systemic administration. *Nature* 522:340–344.
28. Peelaerts W, Baekelandt V (2016) α-Synuclein strains and the variable pathologies of synucleinopathies. *J Neurochem* 139:256–274.
29. Gilman S, et al. (2008) Second consensus statement on the diagnosis of multiple system atrophy. *Neurology* 71:670–676.
30. National Research Council (2011) *Guide for the Care and Use of Laboratory Animals* (National Academies Press, Washington, DC), 8th Ed.

Supporting Information

Woerman et al. 10.1073/pnas.1719369115

SI Materials and Methods

Tissue Homogenization and PTA Precipitation. Fresh-frozen human and mouse brain tissue was used to create a 10% (wt/vol) homogenate in DPBS using the Omni Tissue Homogenizer (Omni International). Samples were aliquoted and stored at −80 °C. Aggregated protein was isolated from patient samples using sodium PTA (Sigma) as described (1, 2). Isolated protein pellets were stored at 4 °C.

Mouse Inoculations. Lysate inoculations were performed using 30 μg total protein diluted in 5% (wt/vol) BSA in DPBS. MSA inoculations were performed using crude brain homogenate diluted to 1% in 5% BSA. Ten-week-old mice were anesthetized with isoflurane before inoculation into the right parietal lobe using a 27-gauge syringe. Following inoculation, all mice were assessed twice each week for the onset of neurological signs based on the standard diagnostic criteria for prion disease (3). Mice were killed within 2 d of demonstrated CNS dysfunction; their brains were then removed and bisected down the midline. The left hemisphere was frozen for biochemical analysis, and the right hemisphere was fixed in formalin for neuropathological assessment.

Immunohistochemistry and Neuropathology. Mouse brains were fixed in 10% (vol/vol) formalin and cut into four sections before processing through graded alcohols, clearing with xylene, infiltrating with paraffin, and embedding. Thin slices (8 μm) were cut, collected on slides, deparaffinized, and exposed to heat-mediated antigen retrieval with citrate buffer (0.1 M, pH 6) for 20 min. Slides from mice inoculated with lysate were stained using a Thermo Fisher Autostainer 480S with 30-min blocking in 10% (vol/vol) normal goat serum and incubation with primary antibody (2 h) and secondary antibody (2 h). Slides from mice inoculated with human samples were stained on the bench with 1-h blocking in 10% normal goat serum and overnight incubation with primary antibody (both at room temperature). Secondary antibody incubation was at room temperature for 2 h. Primary antibodies used include EP1536Y (pS129; 1:1,000; Abcam), glial fibrillary acidic protein (GFAP; 1:500; Abcam), p62 (anti-SQSTM1; 1:1,000; Abcam), and ubiquitin (Ubi1; 1:5,000; Millipore). Secondary antibodies conjugated to Alexa Fluor 488, 568, or 647 (1:500; Thermo Fisher) were used. Slides were imaged using the Zeiss AxioScan.Z1 slide scanner. A positive control was included in all batches of immunostaining.

Digital images of each slide were analyzed using the Zen Analysis software package (Zeiss). A pixel intensity threshold was determined for EP1536Y based on the control slide and was applied to all slides from an experiment. Regions of interest were drawn around the hippocampus, thalamus, hypothalamus, midbrain, and pons, and the percentage of pixels positive for staining in each region was determined. For lysate inoculations, two consecutive sections were cut and analyzed from each mouse, and the average percent area was calculated.

PK Digestion. Brain homogenates were tested for resistance to PK (Thermo Fisher) as described (4). To test PK digestion of α-synuclein fibrils, fibrils were diluted to 200 μg/mL in 1× DPBS for a final volume of 25 μL. PK was added (0, 0.5, 1, 2.5, and 5 μg/mL), and samples were incubated at 37 °C with shaking for 30 min. The reaction was stopped with a final concentration of 5 mM PMSF (Sigma). Samples treated with PK were centrifuged at 100,000 × *g* for 1 h at 4 °C. NuPAGE lithium dodecyl sulfate (LDS) loading buffer (Thermo Fisher) was added to a final volume of 1× with β-mercaptoethanol (BME; Sigma) and 1× NuPAGE reducing agent (Thermo Fisher).

GnHCl Denaturation. GnHCl denaturation of brain homogenates was performed after extracting nine volumes of 10% (wt/vol) brain homogenate in one volume of 10× detergent buffer [5% (vol/vol) Nonidet P-40, 5% (wt/vol) sodium deoxycholate (DOC) in DPBS] on ice for 20 min. Homogenates were centrifuged at 1,000 × *g* for 5 min, and 20 μL of the supernatant was incubated with 0, 1, 1.5, 2, 2.5, or 3 M GnHCl (Sigma) for 2 h at 22 °C with shaking in a final volume of 40 μL. The GnHCl concentration was adjusted to 0.4 M using 1× DPBS, and a final concentration of 1× detergent buffer [0.5% (vol/vol) Nonidet P-40, 0.5% (wt/vol) DOC in DPBS] was added. Sarkosyl (Sigma) was added to a final concentration of 2% (vol/vol). Samples were centrifuged at 100,000 × *g* for 1 h at 4 °C. The supernatant was aspirated, and pellets were resuspended in 40 μL 1× NuPAGE LDS loading buffer and were boiled for 10 min before immunoblotting.

GnHCl denaturation of α-synuclein fibrils was performed by diluting the fibrils to 200 μg/mL in a final volume of 20 μL 1× DPBS. Fibrils were incubated with 0, 1, 1.5, 2, 2.5, or 3 M GnHCl for 2 h at 22 °C with shaking. Additional 1× DPBS was used to dilute the final GnHCl concentration to 0.4 M. Samples were centrifuged at 100,000 × *g* for 1 h at 4 °C. The supernatant was aspirated, and pellets were resuspended in 40 μL 1× NuPAGE LDS sample loading buffer containing BME and 1× NuPAGE reducing agent.

Immunoblotting. PK and GnHCl samples were loaded onto a 10% Novex Bis-Tris gel (Thermo Fisher). SDS/PAGE was performed using the MES buffer system. Protein was transferred to a PVDF membrane. Membranes were blocked in blocking buffer [5% (wt/vol) nonfat milk in 1× Tris-buffered saline containing 0.05% (vol/vol) Tween 20 (TBST)] for 1 h at room temperature. Primary antibody incubation (EP1536Y; 1:4,000; Abcam) was in blocking buffer overnight at 4 °C. Membranes were washed three times with 1× TBST before incubation with horseradish peroxidase-conjugated goat anti-rabbit secondary antibody (1:10,000; Bio-Rad) diluted in blocking buffer for 1 h at room temperature. After blots were washed three times in 1× TBST, membranes were developed using the enhanced chemiluminescent detection system (GE Healthcare) for exposure to X-ray film. GnHCl blots were analyzed using ImageJ, using the 0 M GnHCl sample to standardize the data.

Lysates (1 mg/mL total protein) were loaded onto a 10% Bolt Bis-Tris gel, and SDS/PAGE was performed using the MES buffer system. Protein was transferred to a nitrocellulose membrane. The membrane was blocked in Odyssey blocking buffer (LI-COR) for 1 h at room temperature. Incubation with anti-vinculin (1:10,000; Abcam) and anti-GFP (1:5,000; Rockland) was in Odyssey block buffer with 0.2% Tween 20 overnight at 4 °C. Membranes were washed three times with 1× TBST before incubation with near-infrared secondary antibodies (IRDye goat anti-mouse-680RD and IRDye goat anti-rabbit-800CW, respectively; 1:20,000; LI-COR) diluted in Odyssey block buffer with 0.2% Tween 20 and 0.1% SDS for 1 h at room temperature. After the blot was washed three times in 1× TBST, the membrane was washed a final time in 1× TBS before imaging using the Odyssey Fc (LI-COR).

Silver Staining. Samples were loaded onto a 10% Bolt Bis-Tris gel (Thermo Fisher), and SDS/PAGE was performed using the MES

buffer system. The gel was incubated in fixative [50% methanol and 12% glacial acetic acid (vol/vol)] overnight. After the gel was washed for 30 min in SDS removal buffer [10% ethanol and 5% glacial acetic acid (vol/vol)], it was incubated in Farmer's solution (4.5 mM potassium ferricyanide, 19 mM sodium thiosulfate, and 4.7 mM sodium carbonate) for 2 min. The gel was washed three times for 5 min in double-distilled H_2O and incubated in 12 mM silver nitrate for 20 min. Following a 40-s rinse in milliQ H_2O, the gel was developed in 0.3 M sodium carbonate with 0.0005% (vol/vol) formaldehyde and incubated in stop solution [10% (vol/vol) glacial acetic acid] for 30 min before imaging. The gel was imaged using a ChemiDoc (Bio-Rad). All chemicals were purchased from Sigma.

Statistical Analysis. Data are presented as mean ± SD. Statistical analysis assessing infection of MSA patient samples in the α-synuclein–YFP cell assays was performed using a one-way ANOVA with a Dunnett's multiple-comparison post hoc test. Statistical analysis comparing the onset of neurological symptoms in mice was compared using a log-rank (Mantel–Cox) test to assess the distribution of survival curves. Statistical analysis of data collected from the α-syn140*A53T–YFP cell assay from mice inoculated with cell lysates and patient samples was analyzed using a one-way ANOVA with a Dunnett's multiple-comparison post hoc test. Mouse neuropathology was analyzed using a two-way ANOVA with a Dunnett's multiple-comparisons test comparing each mean with the control sample. Significance was determined with a P value < 0.05.

Data Sharing Statement. All relevant data are presented in the article and *Supporting Information*. The HEK293T cells expressing α-synuclein–YFP are available upon request.

1. Safar J, et al. (1998) Eight prion strains have PrP^{Sc} molecules with different conformations. *Nat Med* 4:1157–1165.
2. Woerman AL, et al. (2015) Propagation of prions causing synucleinopathies in cultured cells. *Proc Natl Acad Sci USA* 112:E4949–E4958.
3. Carlson GA, et al. (1986) Linkage of prion protein and scrapie incubation time genes. *Cell* 46:503–511.
4. Woerman AL, et al. (October 23, 2017) Kinetics of human mutant tau prion formation in the brains of 2 transgenic mouse lines. *JAMA Neurol*, 10.1001/jamaneurol.2017.2822.

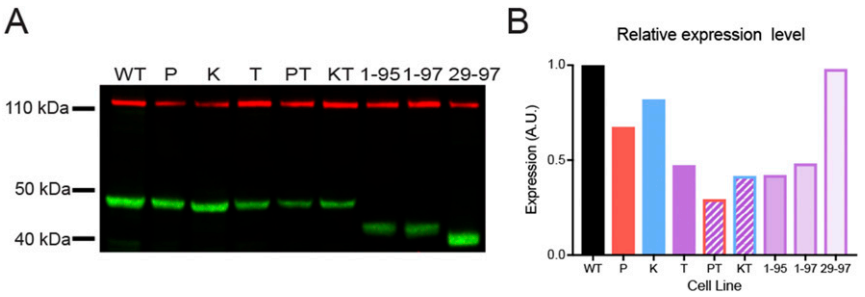

Fig. S1. Protein expression in α-synuclein–YFP cells. (*A*) Lysates were collected from the nine α-synuclein–YFP cell lines (abbreviations are given in Table S1), and expression of each fusion protein was visualized by Western blot probing for GFP (green). The loading control (vinculin) is shown in red. (*B*) Quantification of α-synuclein–YFP expression relative to the WT cell line.

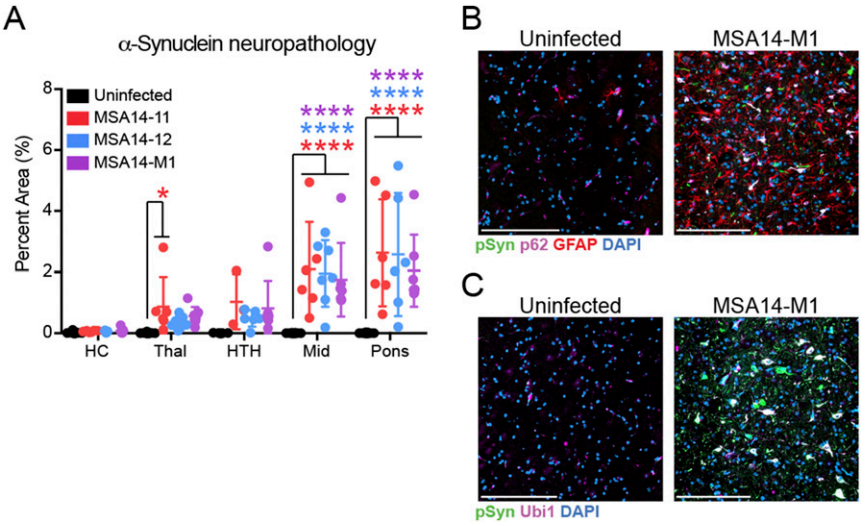

Fig. S2. Neuropathology in mice inoculated with MSA-derived cell lysates. Lysates from α-synuclein–YFP cells infected with MSA prions and from uninfected cells were inoculated into $TgM83^{+/-}$ mice (30 μg protein). (*A*) Phosphorylated α-synuclein neuropathology was quantified in the hippocampus (HC), thalamus (Thal), hypothalamus (HTH), midbrain (Mid), and pons of sick $TgM83^{+/-}$ mice and control animals. Data are shown as mean ± SD. *$P < 0.05$, ****$P < 0.0001$. (*B* and *C*) Representative images of α-synuclein neuropathology (EP1536Y; green). Coronal half-brain sections were imaged using the Zeiss Axio Scan.Z1 within a defined region of interest. Full sections were stitched together using the DAPI channel as a reference. α-Synuclein neuropathology coincided with an increase in astrogliosis (GFAP; red in *B*) in the brainstem of mice inoculated with cell-passaged MSA but not in control animals. α-Synuclein neuropathology was present in the cell bodies and neurites of infected neurons, and it colocalized with p62 (violet in *B*) and ubiquitin (Ubi; violet in *C*) in symptomatic animals; colocalization is shown in white, and nuclei (DAPI-stained) are shown in blue. (Scale bars, 200 μm.)

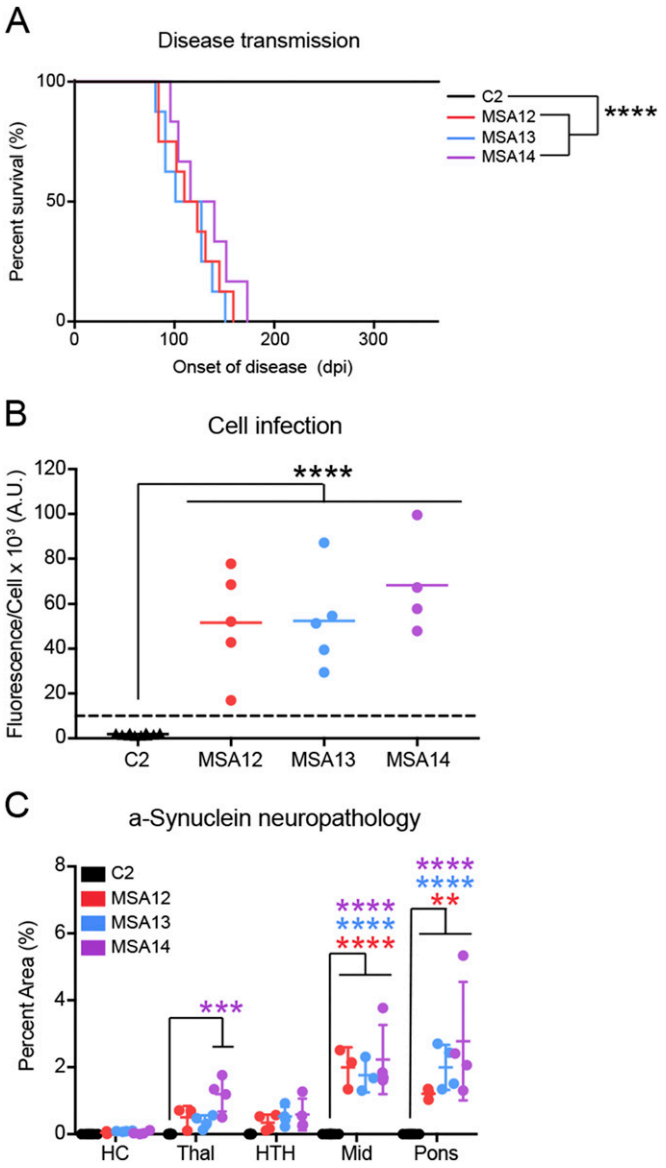

Fig. S3. Transmission of MSA prions to TgM83$^{+/-}$ mice. TgM83$^{+/-}$ mice were inoculated with crude homogenate prepared from one control and three MSA patient samples. (*A*) The Kaplan–Meier plot shows the onset of neurological signs following inoculation; incubation times for MSA12 and MSA13 (1) and MSA14 (2) were previously reported. (*B*) Brains from all mice were tested in the α-syn140*A53T–YFP cell assay (× 10^3 a.u.). Mice inoculated with MSA contained prions (circles above the dotted line). Asymptomatic control-inoculated mouse brains did not contain prions (black triangles below the dotted line). MSA-inoculated mice contained more α-synuclein prions than controls. (*C*) Phosphorylated α-synuclein neuropathology was quantified in the hippocampus (HC), thalamus (Thal), hypothalamus (HTH), midbrain (Mid), and pons of inoculated TgM83$^{+/-}$ mice. Data are shown as mean ± SD. $^{**}P < 0.01$, $^{***}P < 0.001$, $^{****}P < 0.0001$.

1. Prusiner SB, et al. (2015) Evidence for α-synuclein prions causing multiple system atrophy in humans with parkinsonism. *Proc Natl Acad Sci USA* 112:E5308–E5317.
2. Woerman AL, et al. (2015) Propagation of prions causing synucleinopathies in cultured cells. *Proc Natl Acad Sci USA* 112:E4949–E4958.

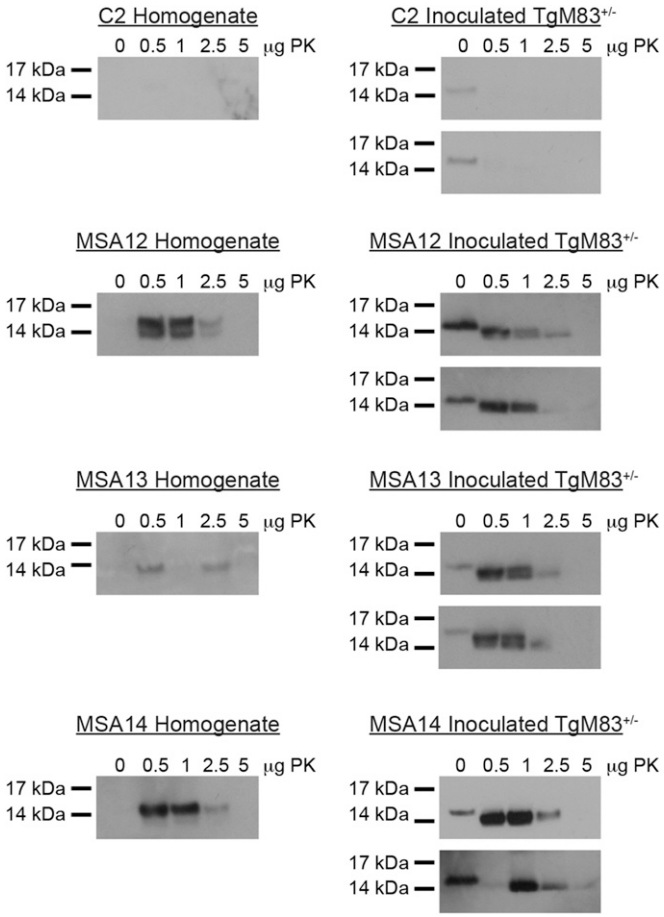

Fig. S4. α-Synuclein in MSA and MSA-inoculated mice is resistant to PK digestion. TgM83$^{+/-}$ mice were inoculated with crude brain homogenate prepared from one control and three MSA patient samples. Frozen half-brains were homogenized in 1× DPBS. Homogenate from the four patient samples (*Left Column*) and the inoculated TgM83$^{+/-}$ mice (*Right Column*) was adjusted to 1 mg of protein and digested with 0, 0.5, 1, 2.5, or 5 μg PK for 30 min. The remaining phosphorylated α-synuclein was detected by Western blot (EP1536Y primary antibody). Homogenate from patient C2 and two mice inoculated with C2 did not contain PK-resistant α-synuclein. Homogenate from the MSA patients and two mice inoculated with each MSA homogenate showed a consistent pattern of PK resistance.

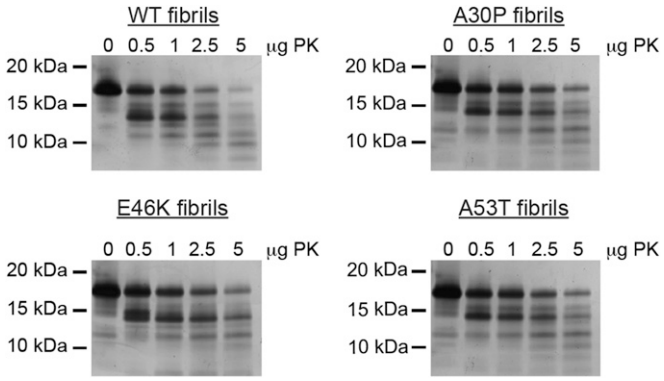

Fig. S5. α-Synuclein fibrils are more resistant to PK digestion than α-synuclein prions in MSA patients. WT and mutated (A30P, E46K, and A53T) α-synuclein was fibrillized in 1× DPBS. Fibrils (200 μg/mL) were digested with 0, 0.5, 1, 2.5, or 5 μg PK for 30 min. The remaining protein was visualized by silver stains, indicating fibrils are resistant to digestion with 5 μg PK.

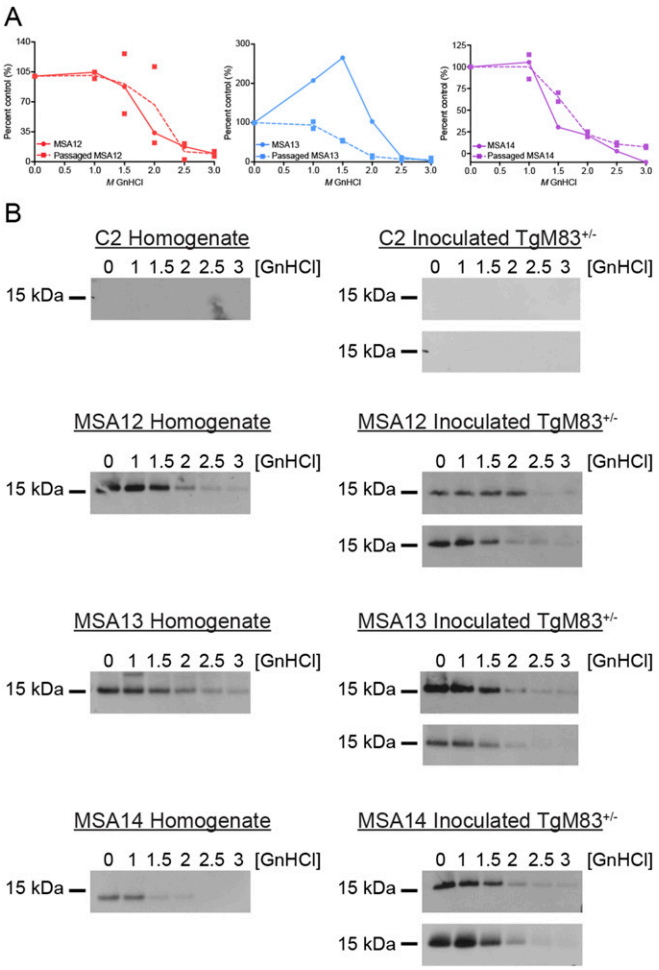

Fig. S6. α-Synuclein in MSA patient samples and mice inoculated with MSA is similarly resistant to GnHCl denaturation. TgM83$^{+/-}$ mice were inoculated with crude brain homogenate prepared from one control and three MSA patient samples. Frozen half-brains were homogenized in 1× DPBS. Homogenate from the four patients and two mice inoculated with each sample was incubated with 0, 1, 1.5, 2, 2.5, or 3 M GnHCl for 2 h. The remaining phosphorylated α-synuclein was detected by Western blot (EP1536Y primary antibody). (*A*) Quantification of phosphorylated α-synuclein in MSA (circles/solid line) and mouse-passaged MSA (squares/dotted line) following GnHCl denaturation. (*B*) Western blots used for analysis in *A*. α-Synuclein was similarly resistant to GnHCl denaturation in two mice inoculated with MSA (*Right*) and in the patient sample (*Left*). Neither control patient tissue nor control-inoculated mice contained phosphorylated α-synuclein following GnHCl denaturation.

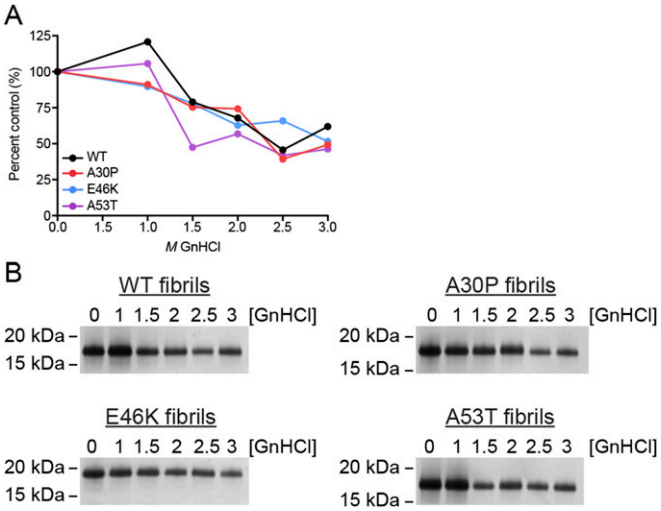

Fig. S7. α-Synuclein fibrils are more resistant to GnHCl denaturation than α-synuclein prions in MSA patients. WT and mutated (A30P, E46K, and A53T) α-synuclein was fibrillized in 1× DPBS. Fibrils (200 μg/mL) were incubated with 0, 1, 1.5, 2, 2.5, and 3 M GnHCl for 2 h. (*A*) Quantification of α-synuclein fibril denaturation using GnHCl indicates 3 M GnHCl, which denatured most α-synuclein in MSA patient samples, degraded only ∼50% of the α-synuclein fibrils. (*B*) Silver stains used for quantification in *A*.

Table S1. α-Synuclein–YFP cell lines

Cell line	Abbreviation	Amino acid residues	Mutations
α-syn140–YFP[†]	WT	1–140	None
α-syn140*A30P–YFP	P	1–140	A30P
α-syn140*E46K–YFP	K	1–140	E46K
α-syn140*A53T–YFP[‡]	T	1–140	A53T
α-syn140*A30P,A53T–YFP	PT	1–140	A30P,A53T
α-syn140*E46K,A53T–YFP	KT	1–140	E46K,A53T
α-syn95*A53T–YFP	1-95	1–95	A53T
α-syn97*A53T–YFP	1-97	1–97	A53T
α-syn29-97*A53T–YFP	29-97	29–97	A53T

[†]Cell line published in Woerman et al (2015) (1).
[‡]Cell line published in Woerman et al (2017) (2).

1. Woerman AL, et al. (2015) Propagation of prions causing synucleinopathies in cultured cells. *Proc Natl Acad Sci USA* 112:E4949–E4958.
2. Woerman AL, et al. (August 28, 2017) MSA prions exhibit remarkable stability and resistance to inactivation. *Acta Neuropathol*, 10.1007/s00401-017-1762-2.

Table S2. Sample infection in α-synuclein cell lines

Sample	Mean cell infection: fluorescence per cell × 10^3 a.u.								
	WT	A30P	E46K	A53T	A30P,A53T	E46K,A53T	1-95*A53T	1-97*A53T	29-97*A53T
C2[†]	1.3 ± 0.6	1.7 ± 0.3	0.6 ± 0.2	1.4 ± 0.2	5.1 ± 1.8	0.3 ± 0.1	0.5 ± 0.1	0.9 ± 0.3	1.0 ± 0.2
MSA12[†]	17 ± 3.3	23 ± 1.4	0.5 ± 0.1	62 ± 7.9	33 ± 5.8	10 ± 1.2	4 ± 0.6	56 ± 9.3	24 ± 4.9
MSA13[†]	54 ± 8.3	76 ± 17	0.5 ± 0.2	85 ± 24	61 ± 11	16 ± 4.1	3.4 ± 0.5	38 ± 8.8	27 ± 1.8
MSA14[†]	17 ± 1.6	25 ± 2.8	0.5 ± 0.1	87 ± 16	31 ± 3.5	4.3 ± 0.6	1.2 ± 0.2	19 ± 7.3	0.7 ± 0.2
C2 → M83[+/−‡]	0.9 ± 0.0	1.4 ± 0.1	0.7 ± 0.1	2.4 ± 0.1	3.6 ± 0.8	0.3 ± 0.0	0.4 ± 0.1	0.5 ± 0.1	0.4 ± 0.0
MSA12 → M83[+/−‡]	18 ± 13	14 ± 6.3	0.6 ± 0.0	45 ± 18	17 ± 15	3.8 ± 3.4	2.0 ± 1.5	21 ± 15	9.9 ± 4.2
MSA13 → M83[+/−‡]	26 ± 0.8	18 ± 1.2	0.8 ± 0.1	47 ± 4.7	29 ± 6.3	4.9 ± 2.3	2.4 ± 0.1	8.2 ± 2.0	13 ± 1.5
MSA14 → M83[+/−‡]	32 ± 7.6	28 ± 8.3	0.9 ± 0.1	64 ± 6.4	36 ± 9.8	7.8 ± 0.8	3.0 ± 1.8	11 ± 2.3	12 ± 0.9
Uninfected lysate[†]	0.7 ± 0.4	0.7 ± 0.2	0.6 ± 0.4	1.1 ± 0.3	3.4 ± 2.8	0.2 ± 0.0	0.4 ± 0.1	0.4 ± 0.2	0.6 ± 0.2
MSA14-11 lysate[†]	4.7 ± 0.8	3.0 ± 0.8	0.6 ± 0.2	60 ± 6.3	17 ± 8.3	8.1 ± 1.0	5.7 ± 0.9	25 ± 1.7	31 ± 6.2
MSA14-12 lysate[†]	4.8 ± 2.0	1.5 ± 0.5	0.9 ± 0.3	43 ± 9.4	7.7 ± 6.4	7.8 ± 6.3	3.9 ± 0.9	16 ± 3.6	16 ± 6.0
MSA14-M1 lysate[†]	12 ± 1.5	9.8 ± 1.5	0.7 ± 0.2	92 ± 19	66 ± 8.3	30 ± 7.8	24 ± 2.2	41 ± 5.8	49 ± 6.6
Uninfected → M83[+/−‡]	1.5 ± 0.7	2.6 ± 0.7	0.8 ± 0.3	2.3 ± 0.4	5.5 ± 2.0	0.4 ± 0.1	1.4 ± 0.2	0.6 ± 0.4	0.9 ± 0.3
MSA14-11 → M83[+/−‡]	51 ± 9.1	35 ± 9.8	1.2 ± 0.5	100 ± 18	54 ± 13	27 ± 9.5	23 ± 14	35 ± 21	60 ± 14
MSA14-12 → M83[+/−‡]	29 ± 16	28 ± 13	1.0 ± 0.4	79 ± 22	46 ± 14	21 ± 9.9	22 ± 12	23 ± 15	45 ± 15
MSA14-M1 → M83[+/−‡]	36 ± 8.2	31 ± 8.5	0.9 ± 0.3	95 ± 15	50 ± 5.1	22 ± 2.9	19 ± 6.8	19 ± 6.1	50 ± 8.2
WT fibrils[†]	180 ± 69	110 ± 37	39 ± 10	330 ± 63	200 ± 22	142 ± 45	49 ± 19	120 ± 25	180 ± 27
A30P fibrils[†]	28 ± 4.2	37 ± 11	33 ± 9.0	53 ± 11	43 ± 4.7	50 ± 9.7	24 ± 4.5	54 ± 22	110 ± 7.5
E46K fibrils[†]	89 ± 31	74 ± 14	97 ± 42	190 ± 47	81 ± 15	230 ± 80	39 ± 7.6	89 ± 27	140 ± 33
A53T fibrils[†]	64 ± 13	48 ± 9.4	26 ± 5.9	190 ± 20	85 ± 13	55 ± 17	28 ± 6.0	55 ± 12	110 ± 24

Data are presented as mean ± SD.

[†]Measurements were made from five images per well, $n = 6$ wells.

[‡]Measurements were made from two mice inoculated with crude homogenate or four mice inoculated with lysate.